Combinatorial Chemical Vapor Deposition of Metal Dioxides Using Anhydrous Metal Nitrates

Ryan C. Smith, Noel Hoilien, Jeff Roberts, Stephen A. Campbell, and Wayne L. Gladfelter*

Departments of Chemistry and Electrical and Computer Engineering, University of Minnesota, Minneapolis, Minnesota 55455

Received October 23, 2001
Revised Manuscript Received December 13, 2001

The search for a dielectric material to replace SiO_2 in field effect transistors has covered many monometallic metal oxides (e.g., TiO_2, ZrO_2, HfO_2, Ta_2O_5, Al_2O_3, etc.) and several compound oxides such as $SrTiO_3$. Silicon nitride and the mixed nitride/oxide of silicon are also candidates.[1,2] Recently, attention has focused on combinations of metal oxides that do not necessarily form a single phase. For example, by co-depositing ZrO_2 with a glass-forming oxide such as SiO_2, one hopes to produce an amorphous, low-leakage current film that still has an acceptably high dielectric constant.[3] Even for a two-component mixture, exploring all compositions becomes a time-consuming task. Using off-axis reactive sputtering, van Dover et al. produced a compositional spread of three metal oxides that allowed a rapid determination of the optimum stoichiometry based on a combination of electrical measurements made on one wafer.[4−6] For the $ZrO_2/SnO_2/TiO_2$ system, this stoichiometry corresponded to $Zr_{0.2}Sn_{0.2}Ti_{0.6}O_2$. Despite the close similarity between the Zr^{4+} and Hf^{4+}, similar experiments established a different ratio ($Hf_{0.2}Sn_{0.05}Ti_{0.75}O_2$) for the hafnium−tin−titanium oxide system.[7]

Reports of using CVD to produce compositional spreads in multicomponent systems have been limited[8,9] and to the best of our knowledge none exist for multicomponent oxides. It is not difficult to design a CVD reactor that could lead to a compositional spread, providing suitable precursors can be found. To achieve precursor compatibility, one would seek to minimize gas-phase reactions and to maintain approximately similar growth rates. This would suggest that we should start with precursors having similar deposition chemistry, that is, similar ligands. In this report we describe the deposition of a compositional spread of HfO_2, SnO_2, and TiO_2 using a modified reactor. The anhydrous metal nitrates of all three metals were known and had been established previously as CVD precursors to the pure metal dioxide films.[10−14]

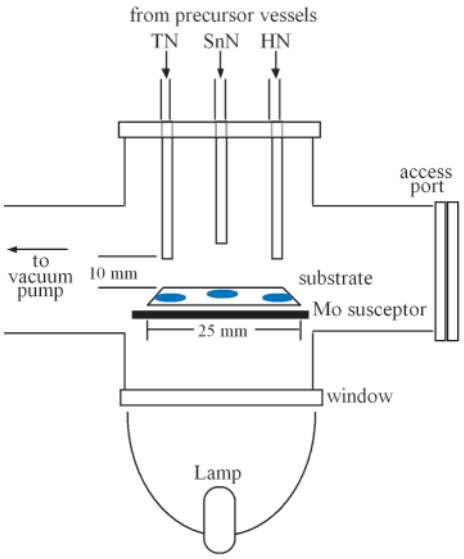

Figure 1. Schematic of the low-pressure, cold-wall CVD reactor showing the precursor inlet arrangement used to obtain the compositional spread. Mass flow controllers regulate the N_2 flow through the precursor vessels containing TN = $Ti(NO_3)_4$, SnN = $Sn(NO_3)_4$, and HN = $Hf(NO_3)_4$. The delivery lines are heated. One of the additional ports of the six-way cross is outfitted with electrical feed throughs for the thermocouples and the other with a window.

The cold-wall, low-pressure CVD reactor, which is described in detail elsewhere,[13] was modified to bring the precursor outlets directly over the substrate at a height of 1 cm (Figure 1). The close proximity of the outlets to the substrate increased the film deposition rates, which were independently measured for each of the single precursors. Approximately equivalent deposition rates were achieved using nitrogen carrier gas flow rates of 15, 10, and 20 sccm through $Ti(NO_3)_4$, $Sn(NO_3)_4$, and $Hf(NO_3)_4$, respectively. The precursor vessels were heated or cooled to 40 °C (for Ti), 0 °C (for Sn), and 60 °C (for Hf), and these conditions led to a reproducible deposition rate of 60 nm/min measured at the center points under each precursor outlet. Wafers were prepared in the routine manner, mounted in the reactor, and heated to 400 °C under nitrogen. The deposition was initiated by simultaneously directing the carrier gas flow through each of the precursor vessels. The total reactor pressure was 0.4 Torr during a deposition. Films

(1) Wilk, G. D.; Wallace, R. M.; Anthony, J. M. *J. Appl. Phys.* **2001**, *89*, 5243−5275.
(2) Buchanan, D. A. *IBM J. Res. Dev.* **1999**, *43*, 245−264.
(3) Wilk, G. D.; Wallace, R. M.; Anthony, J. M. *J. Appl. Phys.* **2000**, *87*, 484−492.
(4) van Dover, R. B.; Schneemeyer, L. F.; Fleming, R. M. *Nature* **1998**, *392*, 162−164.
(5) van Dover, R. B.; Schneemeyer, L. F. *IEEE Electron Device Lett.* **1998**, *19*, 329−331.
(6) Van Dover, R. B.; Schneemeyer, L. F.; Fleming, R. M.; Huggins, H. A. *Biotechnol. Bioeng.* **1999**, *61*, 217−225.
(7) Schneemeyer, L. F.; van Dover, R. B.; Fleming, R. M. *Appl. Phys. Lett.* **1999**, *75*, 1967−1969.
(8) Wang, Q.; Yue, G.; Li, J.; Han, D. *Solid State Commun.* **1999**, *113*, 175−178.
(9) Aiyer, H. N.; Nishioka, D.; Maruyama, R.; Shinno, H.; Matsuki, N.; Miyazaki, K.; Fujioka, H.; Koinuma, H. *Jpn. J. Appl. Phys., Part 2* **2001**, *40*, L81−L83.
(10) Gilmer, D. C.; Colombo, D. G.; Taylor, C. J.; Roberts, J.; Haugstad, G.; Campbell, S. A.; Kim, H. S.; Wilk, G. D.; Gribelyuk, M. A.; Gladfelter, W. L. *Chem. Vap. Deposition* **1998**, *4*, 9−11.
(11) Colombo, D. G.; Gilmer, D. C.; Young, V. G., Jr.; Campbell, S. A.; Gladfelter, W. L. *Chem. Vap. Deposition* **1998**, *4*, 220−222.
(12) Taylor, C. J.; Gilmer, D. C.; Colombo, D. G.; Wilk, G. D.; Campbell, S. A.; Roberts, J.; Gladfelter, W. L. *J. Am. Chem. Soc.* **1999**, *121*, 5220−5229.
(13) Smith, R. C.; Hoilien, N.; Taylor, C. J.; Ma, T.; Campbell, S. A.; Roberts, J. T.; Copel, M.; Buchanan, D. A.; Gribelyuk, M.; Gladfelter, W. L. *J. Electrochem. Soc.* **2000**, *147*, 3472−3476.
(14) Smith, R. C.; Ma, T.; Hoilien, N.; Tsung, L. Y.; Bevan, M. J.; Colombo, L.; Roberts, J.; Campbell, S. A.; Gladfelter, W. L. *Adv. Mater. Opt. Electron.* **2000**, *10*, 105−114.

10.1021/cm011538m CCC: $22.00 © 2002 American Chemical Society
Published on Web 01/12/2002

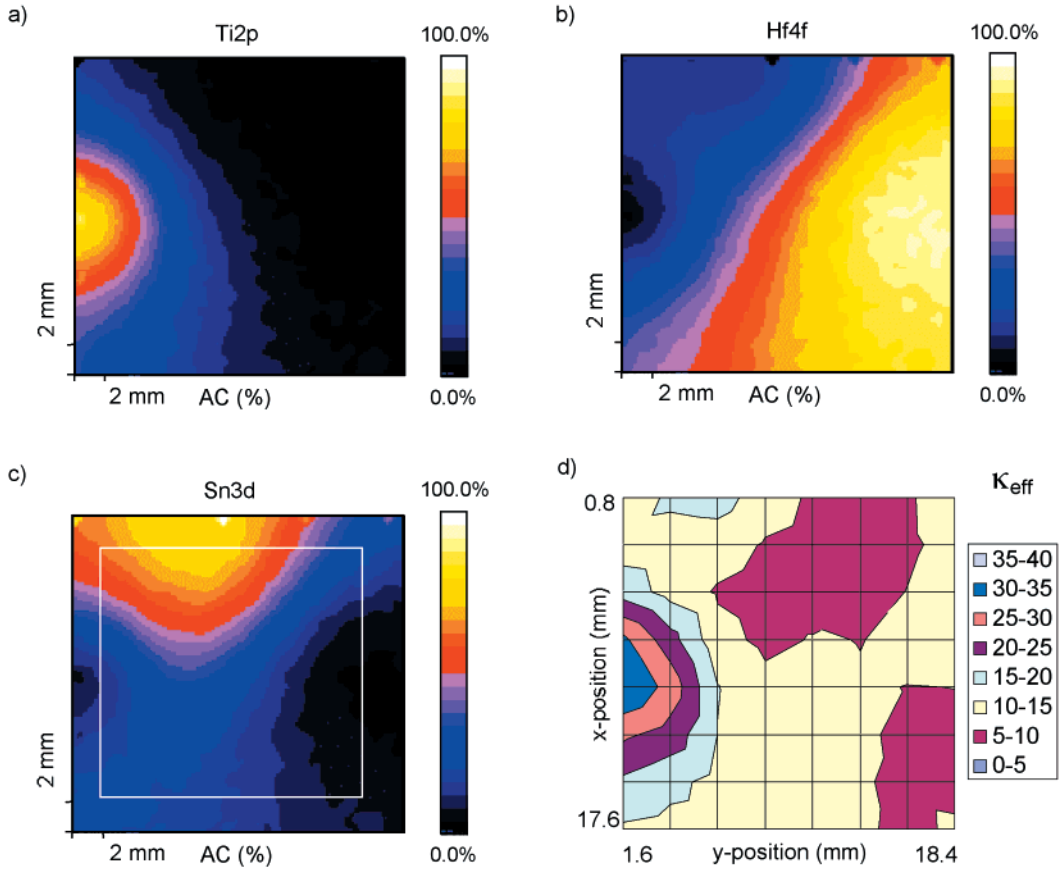

Figure 2. Compositional maps for Ti (a), Hf (b), and Sn (c) derived from a 25 × 25 array of X-ray photoelectron spectroscopic measurements. The percentage is based only on the metal content, and the position scale is shown in the lower left corner of each figure. Figure 2d displays the map of the dielectric constant obtained from the region indicated by the box within 2c. The *x* and *y* positions are measured from the upper left corner of the substrate.

ranging in thickness from 9.5 to 50 nm (this range refers to that found on a single wafer) were used for preparing capacitor arrays and for the X-ray photoelectron spectroscopy (XPS). Thicker films (80−220 nm) were used for Rutherford backscattering spectrometry (RBS) and X-ray diffraction. Ellipsometry was used to measure film thickness for all films, and these results agreed well with the thickness evaluation using RBS. In both the ellipsometry and RBS experiments the beam diameters were 1−2 mm. Capacitor arrays (each capacitor measured 100 × 100 μm) were prepared using standard lithographic methods. The platinum top electrode was deposited by dc sputtering.

X-ray photoelectron spectroscopy (Physical Electronics Quantum 2000 Scanning XPS using monochromatic Al Kα radiation on 625 individual 400 × 400 μm squares) and RBS established that the redesigned reactor produced a compositional spread across the wafer. Figure 2, parts a−c, show the concentrations (in percent) of Ti, Sn, and Hf determined from the intensities of the Hf 4f, Sn 3d, and Ti 2p regions after applying empirical sensitivity factors. The area analyzed by this procedure totaled ≈25% of the sample surface and concentrations of intervening areas were interpolated. To avoid altering of the metal ratios, the XP spectra were obtained without sputter cleaning of the surface. With a t-test, a comparison of the compositions obtained from the 25 × 25 grid of XPS data points with the 6 × 6 grid of RBS measurements established that the methods agreed at a 99% confidence limit. Because RBS provides a measure of the composition throughout the film, we conclude (1) that the surface compositions measured by XPS were representative of those found throughout the film and (2) that the compositional spread was independent of film thickness.

X-ray diffraction of the films was measured using a Bruker AXS microdiffractometer with a 0.8-mm beam diameter. With the exception of the areas immediately beneath the $Ti(NO_3)_4$ and $Hf(NO_3)_4$ outlets, the films were amorphous. In the regions of highest TiO_2 concentration, diffraction from the anatase phase was clearly visible, and broad reflections due to the monoclinic phase of HfO_2 were present in the deposition zone under the hafnium nitrate outlet.

Capacitance−voltage ($C-V$) properties were examined using an HP 4294A impedance analyzer, and current−voltage ($I-V$) measurements were acquired on an HP 4156A parameter analyzer. A square area covering the majority of the sample (see the box indicated in Figure 2c) was selected and the upper left substrate corner was designated as the origin. Both the $C-V$ and the $I-V$ curves were measured from −2 to 2 V. In the absence of an automated system, only a small subset of the ≈30000 capacitors on each chip could be studied. Measurements were performed every 20 capacitors in both *x* and *y* directions, resulting in 64 measurements in an 8 × 8 array. From graphs of the $C-V$ data, the flat band voltage was estimated at the inflection point of the plot. To determine the dielectric constant, the capacitance was measured at a voltage

that was shifted 1.1 V from the flat band voltage toward the region of charge accumulation. Further into the region of accumulation the $C-V$ curves were flat. The effective dielectric constant, κ_{eff}, was calculated using the relationship

$$C = \frac{\kappa_{eff}\epsilon_0 A}{t}$$

where ϵ_0 is the permittivity of free space, A is the area of the capacitor, and t is the film thickness. Figure 2d displays the value of κ_{eff} as a function of position. As observed for the sputter-deposited films exhibiting the same compositional spread of the Ti, Sn, and Hf oxides,[7] the dielectric constant of the film can be estimated by a weighted average of the dielectric constants of the individual oxides. The composition giving the highest κ_{eff} in these CVD-deposited films was $Hf_{0.10}Sn_{0.14}Ti_{0.76}O_2$. Direct comparison to the sputter-deposited films is complicated because the figure of merit used by Schneemeyer et al. was based on the maximum amount of charge stored on a capacitor (=capacitance × breakdown voltage/area). Nevertheless, the highest figure of merit corresponded to $Hf_{0.2}Sn_{0.05}Ti_{0.75}O_2$; thus, both methods suggest a titania-rich film will produce the highest value of κ.

Leakage current densities ranged from 10^{-3} to 10^{-8} A/cm^2. Because more than one charge transport mechanism can be operative, the dependence of leakage current on film thickness cannot be expressed by a single relationship. Empirically, however, we can compare leakage currents across regions of roughly similar thickness. This leads to a rough correlation between increasing leakage current and increasing tin concentration in the dielectric layer. The lowest values of leakage current generally were found in regions of high hafnium concentrations. Additional measurements on thinner films will be needed to quantify more effectively the dependence of the leakage current on composition.

The anhydrous metal nitrates are effective single-source precursors, thus eliminating the need for a secondary source of oxygen such as O_2 or H_2O. Of further value is the observation that the oxide films grown from these precursors can be used without postdeposition annealing under oxygen, thus reducing the thickness of the low κ, SiO_x layer that grows at the interface of the silicon and MO_2 layer. Unlike depositing films by a physical vapor deposition process such as sputtering, we must be concerned about the influence of one precursor and its corresponding oxide on the rate of deposition of the other two. A strong influence might make it difficult to achieve a useful compositional spread. In this study the observation that the combined growth rates of the mixed metal oxides were reasonably predicted on the basis of the growth rates of the individual precursors is important. It suggests that any one of the metal oxides neither poisons nor accelerates the deposition of another. This is at least in part due to the similar deposition chemistry resulting from the common nitrato ligand among the three precursors. For those interested in using CVD in the actual processing environment, these combinatorial experiments are likely to produce compositions, microstructures, and performance more directly related to the scaled-up process.

In summary, we have modified a CVD reactor and deposited a compositional spread of TiO_2, SnO_2, and HfO_2 using the respective anhydrous metal nitrates as single-source precursors. From an array of capacitors, electrical measurements established that the dielectric constant reached a maximum in films having the highest TiO_2 content. This methodology will enable rapid exploration of dielectric properties of multicomponent metal oxide films deposited by CVD, and it is feasible to use the same films to explore the connection between composition and other important physical properties.

Acknowledgment. This research was supported by grants from the National Science Foundation (CHE-0076141) and the Semiconductor Research Corporation.

CM011538M